Temperature Dependence of the Free Volume in Amorphous Teflon AF1600 and AF2400: A Pressure−Volume−Temperature and Positron Lifetime Study

Günter Dlubek,*,† Jürgen Pionteck,‡ Klaus Rätzke,§ Jan Kruse,§ and Franz Faupel§

ITA Institute for Innovative Technologies, Köthen/Halle, Wiesenring 4, D-06120 Lieskau (Halle/S.), Germany; Leibniz Institute for Polymer Research Dresden, Hohe Strasse 6, D-01069 Dresden, Germany; Institute for Materials Research, Chair of Materials Compounds, Faculty of Engineering, Christian-Albrecht-University of Kiel, D-24118 Kiel, Germany

Received April 3, 2008; Revised Manuscript Received June 18, 2008

ABSTRACT: The microstructure of the free volume and its temperature dependence were studied for amorphous Teflon AFs using pressure−volume−temperature experiments (PVT) and positron annihilation lifetime spectroscopy (PALS). Two copolymers of tetrafluoroethylene and 2,2-bis(trifluoromethyl)-4,5-difluoro-1,3-dioxole units with a composition of 35:65 (AF 1600, T_g = 160 °C) and 13:87 mol parts (AF 2400, T_g = 240 °C) were investigated after drying the as-received materials. The results are compared with those for CYTOP (T_g = 105 °C) and the perfluoroelastomer PFE (T_g = −2 °C) as well as for conventional (non-fluorinated) polymers. The PVT data were fitted by the Tait equation and the Simha−Somcynsky (S−S) equation of state (eos). From the latter one the hole fraction h and the specific hole free volume, $V_f = hV$, were determined. From the PALS data published recently by some of the authors (Rudel et al. *Macromolecules* 2008, *41*, 788) the free volume hole size distribution characterized by its mean, $\langle v_h \rangle$, and standard deviation, σ_h, was calculated. The identification of $V_f = N_h' \langle v_h \rangle$ from PALS with $V_f = hV$ from S−S eos opens the way to estimate the specific hole density N_h'. We give evidence for the exceptional large local ($\langle v_h \rangle$, σ_h) and fractional (h) hole free volume in the AF polymers already in the glassy state and relate this to the properties of the particular structure of the heterocyclic dioxole comonomer containing two exocyclic $-CF_3$ groups and to the high dioxole fraction in these copolymers. Correlations between the volume parameters at T_g ($\langle v_{hg} \rangle$, σ_{hg}, and h_g) and the value of T_g or the mass of the S−S mer, respectively, were analyzed. AF2400 shows in some aspects a particularly irregular behavior. Possible limits for the application of the S−S theory to our polymers and complications in interpretation of the PALS data are discussed.

Introduction

Heterocyclic ring-containing fluoropolymers are of special interest for making gas separation membranes due to their particular structure and properties.[1−6] Very famous among this group of polymers are Teflon-AF (DuPont)[2−4] and CYTOP (Asahi Glass).[5,6] Other than polytetrafluoroethylene (PTFE), these polymers are completely amorphous and appear at room temperature in a glassy state. Teflon-AF type copolymers are made from tetrafluoroethylene and 2,2-bis(trifluoromethyl)-4,5-difluoro-1,3-dioxole. They are delivered as Teflon-AF1600 and Teflon-AF2400 with dioxole contents of 65 and 87 mol % and glass transitions at 160 and 240 °C, respectively. These polymers have, although limited, solubility in commercially available perfluorinated ethers and may be solution-cast as films or melt-processed in a variety of forms.

The permeation properties as well as the viscosity, viscoelasticity, the glass transition, volume recovery, and mechanical properties are related to the free volume occurring in amorphous polymers due to their structural disorder. The mobility of small molecules in polymers is closely connected to the hole free volume.[4,7−10] This special type of free volume appears in amorphous polymers in excess to the interstitial free volume, which is observed in polymer crystals, due to their static or dynamic disorder. The hole free volume appears in the form of many irregularly shaped cavities or holes (local free volumes) of atomic and molecular dimension.[7,11−13] The connection between this free volume and the transport of small molecules is described by the theory of Cohen and Turnbull[14,15] and their modifications (ref 7 as an example). The major difficulty in fully assessing any theoretical predictions connecting free volume and molecular mobility is to measure the quantity of the free volume and its microstructure.

In the current work we attempt to characterize the hole free volume in both Teflon AF's as completely as possible and to follow its temperature dependence. To this aim we employ positron annihilation lifetime spectroscopy (PALS)[16−22] and pressure−volume−temperature (PVT)[23] experiments. PALS has developed over recent decades to be the most important experimental method for the study of the free volume in polymers. In this method, positronium (Ps), a hydrogen-like bound electron−positron pair, in its long-lived *ortho* state, *o*-Ps, is used as a probe for subnanometer size local free volumes. The lifetime of *o*-Ps confined in a subnanometer-size hole of the free volume of amorphous polymers mirrors sensitively the size of the hole in which it is annihilated.

PALS experiments on Teflon AF's were already performed in the past by several authors.[4,24−26] Recently, we presented a new series of temperature-dependent PALS measurements of AF1600 and AF2400 (part I of this work[27]). The lifetime spectra were analyzed with the new routine LifeTime in its version LT9.0,[28,29] and the *o*-Ps annihilation rate distribution was determined. We discussed in detail different modes of spectrum analysis such as three- or four-component description of lifetime spectra, implying bimodal or monomodal free volume hole size distribution. Here we focus our discussion on the results from the traditional three-component analysis but involve the distribution of the *o*-Ps annihilation rates. From this distribution the hole volume distribution can be calculated. We characterize the

* To whom correspondence should be addressed: Tel +39-345-5512902; e-mail guenter.dlubek@gmx.de.
† ITA Institute, Köthen/Halle.
‡ Leibniz Institute for Polymer Research Dresden.
§ Christian-Albrechts University of Kiel.

10.1021/ma800748a CCC: $40.75
Published on Web 07/22/2008

temperature dependence of this distribution by the variation of its mean and width.

PALS itself is not able to measure directly the hole density and the hole fraction. However, a correlation of PALS results with PVT experiments allows one to obtain this information.[30–39] In this work we present PVT experiments and fit the data first by the empirical Tait equation[23,40] in the temperature regions above and below $T_g(P)$. The analysis of the PVT data by employing the equation of state (eos) of the Simha−Somcynsky (S−S) lattice−hole theory[41–43] opens the way for an estimation of the fractional hole free volume h. The results of this analysis usually correlate well with the hole volume from PALS and from a comparison the density of holes probed by o-Ps can be estimated.[32–39] The S−S eos is the equation of state which fits usually best the PVT data[44,45] and the only one that allows the explicit calculation of the hole fraction from the volume data. However, in case of the AF polymers we observed larger deviations for medium pressures and higher temperatures. The deviations are similar to those observed by De Angelis et al.[46] when fitting the Sanchez−Lacombe eos to the volume of both AF polymers. We will illuminate possible reasons for these deviations.

In this work we discuss our results for AF1600 and AF2400 in comparison with those for CYTOP, a glassy copolymer, which can be considered to consist of alternating tetrafluoroethylene and hexafluoro-2,3-dihydrofuran units (a pentacyclic structure), and a fraction of a hexacyclic rings (T_g = 105 °C), and for the perfluoroelastomer PFE (Dyneon, a copolymer of tetrafluoroethylene and perfluoro(methyl vinyl ether), see ref 36, T_g = −2 °C). PVT and PALS experiments for these polymers were published by some of us previously.[36–38] Moreover, we study the as-received state of the AF polymers and suggest a treatment to get reproducible results without influence of solvent remnants or overaging.

Experimental Section

As already mentioned, two amorphous Teflon AFs are under investigation: the copolymer of 2,2-bis(trifluoromethyl)-4,5-difluoro-1,3-dioxole and tetrafluoroethylene with the content of the former of 65% (AF 1600) and the copolymer with this content of 87 mol % (AF 2400). The material was delivered by Random Technologies, San Francisco, in the form of 0.1 mm thin foils. We have studied these samples in as-received state and after drying in vacuum.

DSC and PVT experiments were performed using a DSC Q 1000 von TA Instrument (operated with heating and cooling rates of 10 K/min in a nitrogen atmosphere and calibrated by indium and lead standards) and a GNOMIX high-pressure mercury dilatometer, respectively.[23] The GNOMIX instrument is able to detect changes in specific volume as small as 0.0002 cm^3 g^{-1} with an absolute accuracy of 0.004 (below 473 K of 0.002) cm^3 g^{-1}. The polymers were measured between room temperature and 640 K in steps of 5−15 K in standard isothermal mode (ITS) operating between 10 and 200 MPa and recording data in 10 MPa steps. The specific volumes for ambient pressure were obtained by extrapolating the values for 10−30 MPa in steps of 1 MPa according to the Tait equation using the standard GNOMIX PVT software. For calibration of the PVT apparatus the specific volume at environmental conditions must be known. Since the use of a helium pycnometer or the buoyancy method did not result in reproducible density values in case of these highly fluorinated polymers, we determined these values from the filling procedure of the PVT measuring cell, which one can consider as pycnometer with defined volume. The obtained density values of our (dried) samples agreed with those of Angelis et al.[46] with a deviation of not more than 0.3%. Therefore, we have used finally the densities published by Angelis et al.[46] for the calibration of our device: 1.84 g/cm^3 for AF1600 and 1.77 g/cm^3 for AF2400 at T = 35 °C.

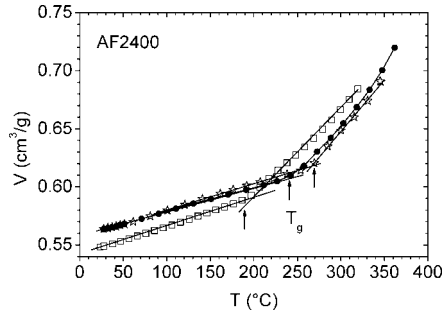

Figure 1. PVT heating curves for Teflon AF2400 at ambient pressure. Shown are the specific volumes for the sample in as-received state (empty squares) and after drying during the first (stars) and second (filled circles) run. The lines are a guide for the eyes.

The as-received samples showed in PVT and DSC experiments (first heat) too low T_gs, which comes according to the data sheets from a plasticization of polymers by low molecular weight solvents used for casting the foils. The second heating scan of DSC showed T_gs near to the expected values and distinct weight losses of samples.

From the filling procedure of the PVT device we calculated for as-received samples a density of 1.880 and 1.816 g/cm^3, which correspond to a plus in density of 2.2% and 2.6% for AF1600 and AF2400, respectively, and a corresponding minus in the specific volume (although the T_g is lower). The lower volumes agree with the PALS results for AF1600, which show a smaller free volume hole size in the first heating run of the as-received sample than in the following cooling run, where it behaves like the carefully dried sample.[27]

To remove the solvents completely, we performed drying of samples in a Büchi furnace in vacuum of 1 mbar with raising temperature in various steps. It needed several days and temperatures near or above T_g to remove finally all solvents. The total weight lost was 8% for AF1600 and 10.5% for AF2400. We remark that CYTOP did not show any effect due the drying procedure. Its DSC glass transition appeared stable at 105 ± 1 °C, independent of the treatments.

After drying of AF1600 both DSC and PVT show the expected value for T_g, 160 ± 2 °C. AF2400 behaves somewhat abnormal. After drying, T_g values of 267 °C (PVT) and 248 °C (DSC) were determined in the first heating run. Probably, some kind of overaging of AF2400 occurs during this long aging period leading to these high T_g values. This overaging effect disappears during the first heating run and is not visible anymore in the following cooling and heating runs as well in DSC as in PVT measurements. The T_g determined from the PVT cooling curve, or a second heating curve, 234 °C, and DSC, second heating run, 237 ± 2 °C, correspond rather to the expected values.

Figure 1 shows the PVT heating curves for Teflon AF2400 in as-received state (specific volume extrapolated to ambient pressure) and after drying during the first and second heating run. The second heat DSC curves shown in Figure 2 exhibit a clear glass transition, which shows that the samples are all in an amorphous, more or less random, copolymer state. As conclusion of our preinvestigations, we dried the samples as described above to constant weight, heated them in the PVT device to 300 °C, cooled down, and started subsequently the PVT runs. The T_g values from these PVT experiments agreed with those from DSC of the second heat of dried samples. PVT heating and cooling runs of samples treated in this way showed almost no hysteresis.

The PALS experiments, spectrum analysis, and lifetime results were discussed in detail in the first part of the work.[27] Here we calculate from the o-Ps lifetime distributions the sizes distributions of the local free volumes and compare these with the free volume parameters derived from the PVT experiments.

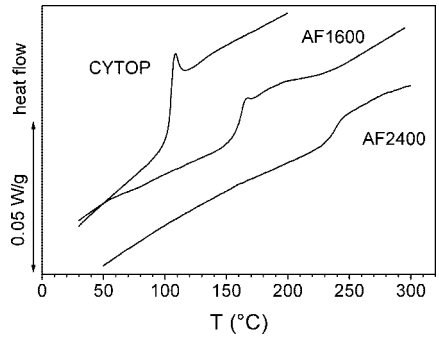

Figure 2. DSC curves for AF2400, AF1600, and, for comparison, CYTOP. Shown are the second heating runs of the dried samples.

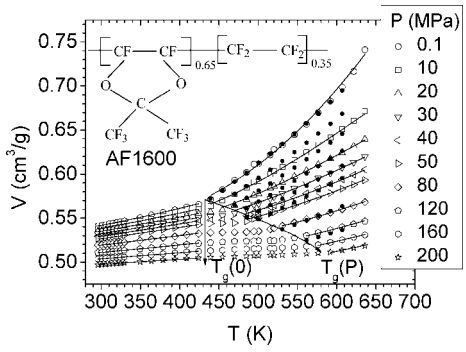

Figure 3. Specific total volume V (empty symbols) as a function of temperature T at a series of constant pressures P for Teflon AF1600. $T_g(0)$ and $T_g(P)$ represent the glass transition temperature at pressures zero and P, respectively. The solid lines show the fits of the Tait equation (eq 1) to the data from below $T_g(0)$ and above $T_g(P)$. The dots show results of fits of the S−S eos (eq 3) to the volume data from the region between $T_g(P)$ and 610 K and 0 and 120 MPa.

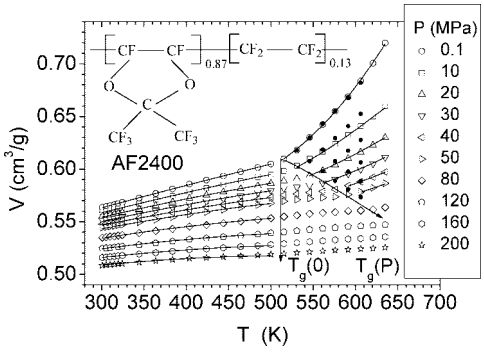

Figure 4. As for Figure 3, but AF2400. The Tait and S−S eos fits above $T_g(P)$ were restricted to the pressure range between 0.1 and 50 MPa.

Results and Discussion

Specific Total and Free Volume from PVT Experiments. Figures 3 and 4 show the temperature dependence of the specific volume of AF1600 and AF2400 for selected pressures and the results of various fits to these data. The pressure-dependent glass transition is indicated by $T_g(P)$. First, we have fitted the PVT data by the empirical Tait equation[23,40]

$$V(P,T) = V(0,T)\{1 - C\ln[1 + P/B(T)]\} \quad (1)$$

with $V(0,T) = \sum C_n T^n$ ($n = 0, 1, 2$) and $B(T) = B_0 \exp(-B_1 T)$. A value of $C = 0.0894$ has been customarily used, following the original analysis of hydrocarbons. Least-squares fits to the experimental volumes from the range $T > T_g(P)$ done with this value of C showed some systematic deviations. Therefore, we allowed C to vary and got from consecutive fits to the data the parameters shown in Table 1. Fits to the data from the temperature range $T < T_g(0)$ also delivered good results, and the parameters are displayed in the same table. Figures 3 and 4 show these fits as solid lines. The fits were done in the Celsius scale to get the reference volume $V(0)$ for 0 °C, but all data from now are presented in the absolute temperature scale. From eq 1 and the fitted parameters the coefficient of thermal expansion and the compressibility can be easily calculated.

Further fits were performed employing the eos of the S−S lattice−hole theory.[41–43] This theory describes a liquid as a periodic lattice of cells of equal size. The disorder is modeled by assuming a statistical mixture of occupied (fraction y) and unoccupied cells (holes or vacancies, fraction $h = 1 - y$). The S−S eos is represented in scaled form with scaling parameters P^*, V^*, and T^* in two coupled equations. One of these follows from the pressure equation $P = -(\partial F/\partial V)_T$, where $F = F(V, T, y)$ is the configurational (Helmholtz) free energy F of the liquid

$$\tilde{P}\tilde{V}/\tilde{T} = [1 - \eta]^{-1} + 2yQ^2(AQ^2 - B)/\tilde{T} \quad (2)$$

where $Q = (y\tilde{V})^{-1}$, $\eta = 2^{-1/6}yQ^{1/3}$, $A = 1.011$, and $B = 1.2045$. $\tilde{P}$, $\tilde{V}$, and $\tilde{T}$ are the reduced variables, $\tilde{P} = P/P^*$, $\tilde{V} = V/V^*$, and $\tilde{T} = T/T^*$. The occupied volume fraction y is coupled with $\tilde{T}$ and $\tilde{V}$ in a second equation derived from the minimization condition $(\partial F/\partial y)_{V,T} = 0$. It was shown that both equations may be replaced in the temperature and pressure ranges $\tilde{T} = 0.016-0.071$ and $\tilde{P} = 0-0.35$ by the universal interpolation expression

$$\ln \tilde{V}(P,T) = a_0 + a_1\tilde{T}^{3/2} + \tilde{P}[a_2 + (a_3 + a_4\tilde{P} + a_5\tilde{P}^2)\tilde{T}^2] \quad (3)$$

The scaling parameters are related to the molar mass of the S−S mer via $M_0 = (c/s)RT^*/P^*V^*$, where R is the gas constant, s is the mean number of mers of the S−S lattice (s-mers) in a chain, and $3c$ is the number of external degrees of freedom per molecule. For polymers, $s \to \infty$, and a single external degree of freedom of a S−S mer, $3c/s = 1$, is assumed. This fixing defines M_0 and its ratio to the mass of the chemical repeat unit, M_{rep}. The constants in eq 3, following the most recent determination,[40] are $a_0 = -0.10346$, $a_1 = 23.854$, $a_2 = -0.1320$, $a_3 = -333.7$, $a_4 = 1032.5$, and $a_5 = -1329.9$.

Simultaneous fits to all data from the range $T > T_g(P)$ showed that eq 3 does not well describe the whole PVT surface. The deviations go into the same direction but are stronger than those observed for CYTOP.[38] Since we are mostly interested in a perfect fit to the ambient pressure data (for comparison with the PALS data), we have used again consecutive fits and restricted the fitting range to the data from the region between $T_g(P)$ and 610 K and 0.1 and 120 MPa (AF1600) or 50 MPa (AF2400), respectively. Figures 3 and 4 show these fits as dots. The data at ambient pressure are well described by this eos and the scaling parameters V^* and T^* depend only slightly on the temperature range used for fitting. At medium pressures and higher temperatures the volume appears more compressible than described by the S−S theory. The fitting parameter P^* depends more strongly on the selected pressure range. The uncertainty of ±50 MPa given in Table 2 is a statistical error of the fit and does not include possible systematic errors.

Table 2 displays together with the parameter from the S−S eos fits several other values calculated from these data, supplemented by the results for CYTOP and PFE. Their meaning and importance were discussed in detail in previous publications.[32–43] The fraction of unoccupied lattice sites (vacancies of the S−S lattice) $h = 1 - y$ can be calculated for the glassy and the rubbery states of polymers from a numerical solution of eq 2 using the scaling parameters estimated for the equilibrium state. Arguments for the validity of this procedure for the (nonequilibrium) glass were given in earlier papers.[42]

Table 1. Results from the Tait Analysis of PVT Data of Teflon AF1600 and AF2400

	AF1600		AF2400	
polymer	glass	rubber	glass	rubber
C_0 ($cm^3\ g^{-1}$)	0.5370 ± 0.001	0.5494 ± 0.008	0.5574 ± 0.002	0.649 ± 0.02
C_1 ($cm^3\ g^{-1}\ °C^{-1}$)	$(1.70 \pm 0.04) \times 10^{-4}$	$(-1.4 \pm 0.7) \times 10^{-4}$	$(2.2 \pm 0.05) \times 10^{-4}$	$(-8.8 \pm 0.4) \times 10^{-4}$
C_2 ($cm^3\ g^{-1}\ °C^{-2}$)	$(1.6 \pm 0.3) \times 10^{-7}$	$(1.80 \pm 0.1) \times 10^{-6}$	$(-4.79 \pm 2.2) \times 10^{-8}$	$(2.97 \pm 0.2) \times 10^{-6}$
C	0.0943 ± 0.001	0.0760 ± 0.001	0.0892 ± 0.0006	0.0781 ± 0.001
B_0 (MPa)	161.3 ± 2.5	256 ± 16	112.75 ± 1.2	978 ± 50
B_1 ($°C^{-1}$)	$0.00374 \pm 0.000\ 03$	0.0113 ± 0.0003	$0.00361 \pm 0.000\ 02$	0.0145 ± 0.0002
R^2	0.9998	0.9990	0.9996	0.9996

Table 2. Results from the S−S eos Analysis of PVT Data of Teflon AF1600 and AF2400[a]

quantity	uncertainty	PFE	CYTOP	AF1600	AF2400
T_g (DSC, K)	±2	271	378	433	510
T_g (PVT, K)	±3	n.d.	369	435	515
T^* (K)	±40	8038	9332	7926	7541
V^* (cm^3/g)	±0.001	0.4501	0.4624	0.4649	0.4390 (0.4648)
V^*/V_w		1.503	1.559	1.533	1.442 (1.52)
P^* (MPa)	±50	749	664	507	489
$\langle M_{rep}\rangle$ (g/mol)[e]		123.1	139.03	193.6	225.3
M_0 (g/mol)	±10	63.2	88.6	98.1	102.0
v_{SS} (Å^3)[b]	±0.5	45.2	64.7	71.8	69.5 (72.8)
V (cm^3/g)[b]	±0.002	0.4811	0.4929	0.5415	0.5636
V_w (cm^3/g)[e]		0.2994	0.2965	0.3032	0.3044
$f_w = 1 - V_w/V(T)$[b]	±0.001	0.378	0.397	0.438	0.460
V_{occ} (cm^3/g)[b]	±0.003	0.4310	0.4394	0.4408	0.4105 (0.430)
V_f (cm^3/g)[b]	±0.003	0.051	0.0534	0.101	0.153 (0.133)
h[b]	±0.003	0.105	0.108	0.186	0.272 (0.237)
$h_g = h(T_g)$	±0.003	0.084	0.118	0.210	0.305 (0.270)
$\alpha_g(h)$ ($10^{-3}\ K^{-1}$)	±0.05	n.d.	1.27[c]	0.93[c]	0.60[c]
$\alpha_r(h)$ ($10^{-3}\ K^{-1}$)	±0.1	7.3[b]	5.79[d]	3.61[d]	2.61[d]

[a] For explanation of symbols see text, and for the fitting ranges in T and P see text and refs 36–38; the numbers in parentheses are estimated from eq 4. [b] At 296 K. [c] For $T < T_g$ and $T \rightarrow T_g$. [d] For $T > T_g$ and $T \rightarrow T_g$. [e] Mole parts weighted average.

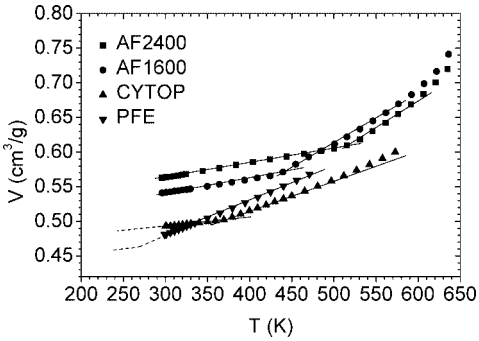

Figure 5. Specific total volume V as a function of temperature T at ambient pressure for several fluoropolymers. The solid lines are linear fits to the data from below T_g and from the temperature range between $T_g + 10$ K and $T_g + 60$ K. The dashed lines show the expected behavior of V from an extrapolation.

Figures 5 and 6 show the temperature dependency of the specific volume V and the hole free volume fraction h at ambient pressure for the four polymers under discussion. The data in Table 2 show, that when going from PFE to AF2400, the ratio V/V_w increases at 296 K from 1.61 to 1.85. The mean van der Waals volume per gram of the copolymers, V_w, was determined from the ratio $\langle V_w\rangle/\langle M_{rep}\rangle$, where $\langle V_w\rangle$ and $\langle M_{rep}\rangle$ are the mean molar van der Waals volume and mean weight of the repeating unit calculated as mole fraction weighted averages. These values were calculated from the group contributions tabulated by van Krevelen.[47] Correspondingly to V/V_w, the total or van der Waals free volume fraction increases from $f_{total} = 1 - V_w/V = 0.378$ to 0.460. The hole fraction determined from the S−S eos is less than this value, $h = 0.105-0.272$, while its part in the total free volume increases from $h/f_{total} = 0.28-0.59$. The specific volume calculated from $V_f = hV = V - V_{occ}$ ($V_{occ} = yV = (1 - h)V$) represents the sum of the volumes of all unoccupied lattice cells (vacancies) in a gram of the polymer which we, therefore, denote as hole free volume. Within the occupied cells the free volume $V_{fi} = V_{occ} - V_W$ appears, which may be denoted as interstitial free volume. The volume of a cell of the S−S lattice is given by $v_{SS} = M_0V_{occ}/N_A$, where N_A is Avogadro's number.

Our data give evidence for the extraordinary larger hole free volume of the copolymers of tetrafluoroethylene. This is in particular true for the AF polymers which can be attributed to a stiffening of the macromolecular chain by the heterocyclic-ring-containing fluorocomonomers. The glass transition is clearly seen as a change in the coefficient of thermal expansion of the total (Figure 5) and hole free volume, $\alpha(h) = (1/h)(dh/dT)|_P$ (Figure 6), at the temperature T_g(PVT) (Table 2). While the gradient dh/dT is almost same for the various polymers, the coefficient $\alpha(h)$ decreases from PFE to AF2400 due to the increasing values of $h_g = h(T_g)$. In case of AF2400 the h values increase from 0.27 at 300 K to 0.38 at 610 K. Conventional polymers show typically changes of h between 0.02 and 0.2. For PFE a value of $h_g = 0.084$ follows from an extrapolation to $T_g = 271$ K.[36]

For an attempt to systematize the hole fraction at T_g, h_g, we have plotted in Figure 7 this value as a function of T_g and of M_0, the molecular weight of the S−S mer, respectively. The plot involves "conventional" polymers (those without cyclic or linear fluorine groups in the main chain)[48] and VDF/HFP22, a copolymer of vinylidene fluoride (78 mol %) and hexafluoropropylene (22 mol %).[36] The h_g values of the fluoropolymers increase roughly linearly with T_g (dotted line in Figure 7), $h_g = -0.20(\pm0.05) + 9.5(\pm2) \times 10^{-4}T_g$ (K), starting from an extrapolated zero at $T_g = 210$ K. We note that this dependence is much steeper than observed for conventional polymers, $h_g = -0.0165(\pm0.02) + 2.3(\pm0.1) \times 10^{-4}T_g$ (K) or, more accurately, $h_g = 5.32(\pm0.3) \times 10^{-7}T_g^2$ (K) (solid line in Figure 7).[32,46] These dependencies show that for high-T_g polymers a large hole fraction is required to pass into the rubbery state. Our copolymers with cyclic fluorine groups, however, show the peculiarity that they exhibit up to 2 times larger hole fractions at comparable T_g than conventional polymers. This indicates that the h_g-T_g correlation is not universal for all types of polymers but is affected by their chemical structure.

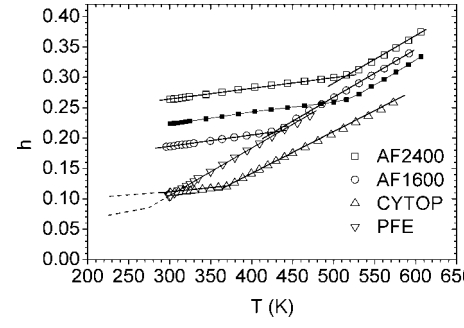

Figure 6. As for Figure 5, but the fractional hole free volume h calculated from the S−S eos eq 2 (empty symbols). The small filled squares show a values for AF2400 calculated on a different way (see text, eq 4).

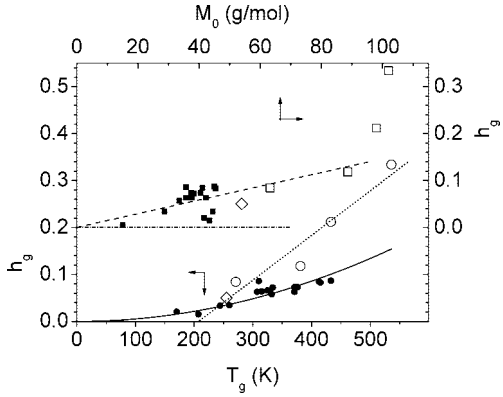

Figure 7. Hole free volume fraction at T_g, h_g vs T_g (circles) and vs the molecular weight of the mer of the S−S lattice, M_0, calculated from the PVT data (squares): open symbols, our fluoropolymers; diamonds, VDF/HFP22, from ref 36; filled symbols, conventional polymers, from ref 48. The statistical error for M_0 is in the order of ±5% and that of h_g less than 0.005. The dashed line shows a linear and the solid line a quadratic fit to the data for conventional polymers constrained to pass zero. The dotted line shows a linear fit to the h_g vs T_g data for the fluoropolymers.

In this context we mention that the molecular weight of the S−S mer, M_0, of our fluoropolymers varies approximately linearly with T_g, M_0 (g/mol) = 16(±12) + 0.175(±0.03)T_g (K) or, more roughly, M_0 (g/mol) = 0.213(±0.02)T_g (K). Correspondingly, the S−S cell size changes like v_{SS} (Å^3) = 0.187(±0.01)T_g (K). Again, these variations are distinctly stronger than for conventional polymers, where M_0 shows only a slight increase with T_g, M_0 (g/mol) = 35(±9) + 0.014-(±0.02)T_g (K). Apparently, the mean molecular weight of the S−S mer mirrors to some extent the stiffness of polymer chains. Continuing with this philosophy, the top part of Figure 7 shows the hole fraction h_g vs M_0. A linear fit to the data of the conventional polymers constrained to pass zero gives h_g = 1.4(±0.2) × $10^{-3}M_0$ (g/mol) (dashed line). This dependence describes also the h_g values of VDF/HFP22, PFE, and CYTOP. From this behavior one may conclude that the mer of the S−S lattice has the character of a mobile unit or is closely related to it. It controls to some extent the hole fraction which is required to pass into the rubbery state. The values for both AFs are distinctly above this line, which again shows the importance of their particular chemical structure. We remember that the ring in the CYTOP structure contains, in addition to two CF groups, two (some rings three) CF_2 groups while the dioxole ring of the AF polymers contains two exocyclic CF_3 groups. We expect that the latter, bulky, group is largely responsible for the extraordinary high free volume of the AFs in comparison to CYTOP, the other heterocyclic-ring-containing copolymer.

At this point we like to critically review possible error sources in the calculation of the hole fraction h which may come from an inadequate application of the S−S eos to the heterocyclic copolymers being under investigation in this work. The non-perfect fitting of the PVT data of our AF polymers in the whole range of temperatures and pressures may mirror some feature of these polymers that prevents it from being accurately described by the S−S theory. We recall that the S−S statistical thermodynamics theory[41–43] assumes a single-component system (either a homopolymer or multicomponent system with averaged parameters) with (in case of polymers) linear molecular chains which have a number of interchain nearest neighbors or intermolecular contact sites of $qz = s(z - 2) + 2$. s is the mean number of s-mers in a chain molecule, and z = 12 is the coordination number in the quasi-lattice. The number of external (i.e., volume-dependent) degrees of freedom of a s-mer is a parameter of the eos which for polymers is usually assumed to be 1; i.e., the energy barriers for internal bound rotation are low in comparison with intermolecular effects (an ideally flexible chain). The intermolecular potential is described by a 6−12 Lennard-Jones potential in the square-well approximation. Despite these restricting assumptions in modeling, the S−S theory has been successfully applied to analyze the volumetric behavior of nonlinear polymers[45] and also of copolymers[49] and blends.[50]

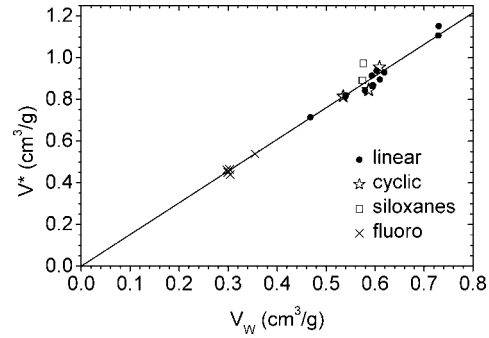

Figure 8. Relation between the S−S eos scaling volume V^* and the van der Waals volume V_w for polymers. Shown are the data for linear polymers, polymers and copolymers which have cyclic groups in the main chain, siloxanes, and fluoropolymers. The line is a linear fit to all data constrained to pass zero, $V^* = 1.520(\pm 0.013)V_w$ (compare ref 52).

In order to get some information on this question, we will compare our estimated scaling parameters with those obtained for conventional polymers. Simha and Carri[51] found a linear relation between the scaling volume V^* and the van der Waals volume V_w: $V^* = 1.45V_w$ for polymers and $V^* = 1.60V_w$ for low molecular weight liquids. The V^* values estimated by Srithawatpong et al.[32] for several polymers correspond to $V^*/V_w = 1.57-1.60$. In Figure 8 we have plotted V^* from previous studies of some of us vs V_w. A linear fit to all data shown in the Figure delivers $V^* = -0.0065(\pm 0.027) + 1.537(\pm 0.05)V_w$ (compare ref 52). A fit constrained to pass zero gives $V^* = 1.520(\pm 0.013)V_w$. Among the non-fluoropolymers polydimethylsiloxane (PDMS, $V^*/V_w = 1.68$) and monomeric and oligomeric diglycidyl ether of bisphenol A (DGEBA, $V^*/V_w = 1.44$, lower star in Figure 8) show the maximum deviations from this line. Figure 8 indicates that the fluoropolymers do not scatter out from this line more than some of the other polymers. The fluoropolymers shown in this figure include polytetrafluoroethylene (PTFE, 1.566) and VDF/HFP22 (1.514). The ratios V^*/V_w of the other fluoropolymers are shown in Table 2. From our heterocyclic copolymers AF2400 scatters mostly out of the fitted line with the ratio of $V^*/V_w = 1.442$.

To estimate possible consequences of this deviation on the hole fraction h, we use the following approximation for its estimation in equilibrium ($T > T_g$):

$$h = [V - K(T/T^*)V^*]/V \tag{4}$$

where $K(T/T^*)$ is a material-independent very slowly varying function of T which has a value of K = 0.958 at the T_g of AF2400.[53] KV^* (=$1.453V_w$) represents the occupied volume which corresponds to the volume typical for polymer crystals, $V_c = 1.45V_w$.[47] It shows almost no temperature dependence above T_g. With V^* = 0.4390 cm^3/g (Table 2) eq 4 delivers h_g = 0.305, in agreement with the numerical calculation from eq 2. Assuming $V^* = 1.52V_w$, one obtains V^* = 0.4648 cm^3/g and from eq 4 h_g = 0.270, which is less than the numerical estimate. Possibly, we must lower the h values of AF2400. In Figure 6 we have tentatively shown the h curve of AF2400 lowered by an amount of 0.035 (by small filled squares) in comparison to that calculated from eq 2. These corrected values of h seem to be in better agreement to the behavior of the

specific volume shown in Figure 5 when comparing AF2400 with AF1600. Below T_g, after this correction V and h are larger for AF2400 than for AF1600, which may be attributed to the larger topologic disorder and the larger chain stiffness in the former polymer. This behavior inverts above T_g due to the thermal expansion and the formation of free volume due to thermal fluctuations (see the discussion in ref 38). An analogous situation can be observed when comparing PFE and CYTOP. We remark that the estimated $V^* = 0.4648$ cm^3/g agrees with the values analyzed for AF1600 and CYTOP (Table 2). V_{occ} of AF2400 estimated from $V_{occ} = KV^*$ is very close to the value of $V_{occ} = yV$ for AF1600 from eq 2. In case of PFE, CYTOP, and AF1600 the values of V^* estimated from eq 2 deviate not much from the fit $V^* = 1.52V_w$. In these cases the numerical estimates for the hole fraction h may well represent the true values.

Temperature Dependence of Hole Volume from PALS. As mentioned, we have presented in an early paper[27] temperature-dependent PALS experiments for AF1600 and AF2400 and discussed different modes of the analysis of positron lifetime spectra. Here we focus our discussion to the results from the three-component analysis using the routine LT9.0.[28,29] In this analysis we allowed the lifetimes of free positrons (component 2) and *o*-Ps (component 3) to show a distribution. Only the *p*-Ps lifetime (component 1) was assumed to appear discrete. This assumptions lead to rather perfect fits to the experimental spectra and involve a smaller number of fitting parameters than four-component fits.[27] We considered these fit parameters as that reasonable result, which can be derived from the experiment within the limits of the experimental accuracy (see the general discussion of the problem of deconvolution, lifetime extraction, and information content for nonexponential decays in refs 54 and 55). Moreover, the results from this type of analysis can be compared with our previous works. The third lifetime component, which comes from the annihilation of *o*-Ps localized at free volume holes, was characterized by the mean, $\tau_3 \equiv \langle\tau_3\rangle$, and the width parameter σ_3 (standard deviation calculated from the square root of the second moment) of the *o*-Ps lifetime distribution and by the *o*-Ps intensity I_3. The *o*-Ps lifetimes show a distribution since the holes show a size (and shape) distribution.

The usual way to calculate the radius r_h of the hole (assumed to be a sphere) where *o*-Ps is localized and annihilated employs the quantum-mechanical equation[56]

$$\lambda_{po} = 1/\tau_{po} = 2\ \text{ns}^{-1}\left[1 - \frac{r_h}{r_h + \delta r} + \frac{1}{2\pi}\sin\left(\frac{2\pi r_h}{r_h + \delta r}\right)\right] \quad (5)$$

where λ_{po} is the mean rate of *o*-Ps pick-off annihilation with electrons of the molecules in the hole walls, $\lambda_{po} = \lambda_3 = 1/\tau_3$. $\delta r = 1.66$ Å is an empirical parameter which describes the overlap of the Ps wave function with the hole walls.[57,58] The hole volume may be calculated from $v_h(\tau_3) = (4/3)\pi r_h^3(\tau_3)$.

The probability density function (pdf) of the hole sizes $n(r_h)$ can be calculated from $n(r_h) = -\alpha_3(\lambda)d\lambda/dr_h$, where $\alpha_3(\lambda)$ is the distribution of the *o*-Ps annihilation rates.[55,59] The routine LT9.0 assumes that $\alpha_3(\lambda)$ follows a logarithmic Gaussian function. It is not very clear whether $n(r_h)$ mirrors a weighted hole size distribution and what the possible weighting factor is. In generally, it is expected that larger holes promote Ps formation and localization. Jean and collaborators have assumed that $n(r_h)$ includes a weighting factor of the type $K(r_h) = 1.0 + 8.0r_h$.[59] We have usually assumed a weighting proportional to the hole volume.[34–38] The hole volume distribution can be calculated from $g(v_h) = n(r_h)/4\pi r_h^2$. The mean and the standard deviation of $g(v_h)$, $\langle v_h\rangle_v$, and σ_{hv} may be then considered as volume-weighted values. The number-weighted distribution is given by $g_n(v_h) = g(v_h)/v_h$. Their parameters $\langle v_h\rangle$ and σ_h and $\langle v_h\rangle_v$ and σ_{hv} as well were calculated as first moment and square-root of the second moment of the corresponding distribution.

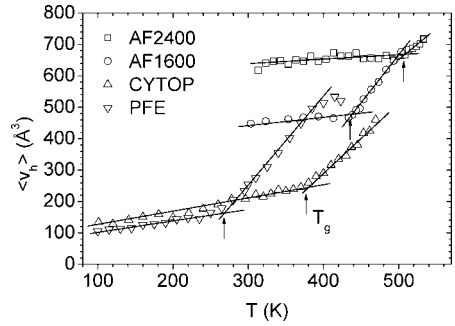

Figure 9. Mean hole volume $\langle v_h\rangle$ calculated from the first momentum of the distribution $g_n(v_h)$ for various fluoropolymers. The lines show linear fits to the data from the temperature ranges below and above T_g under exclusion of the data of PFE from above 400 K.

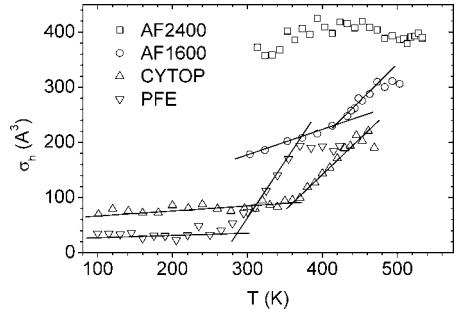

Figure 10. As for Figure 9, but the standard deviation (square root of the second momentum) of the distribution $g_n(v_h)$. The lines are a guide for the eyes.

Figures 9 and 10 show the volume parameters for the four fluoropolymers under discussion in this work. We focus on the comparison to the values $\langle v_h\rangle$ and σ_h derived from the distribution $g_n(v_h)$. Table 3 displays the parameters determined from these plots. The glass transition is seen as a jump in the slope of the $\langle v_h\rangle$ and σ_h plots. At higher temperatures frequently a leveling-off of the increase in the mean hole volume is observed, which can be attributed to relaxation times of structural relaxation shorter than the *o*-Ps lifetime. The leveling-off occurs also in the mean dispersion of the distribution (at somewhat lower temperatures) and was interpreted to be due to the disappearance of the dynamic heterogeneity of structural relaxation. These effects are most clearly seen for PFE (see the discussion in refs 36, 37, and 60).

The results show that AF1600 and AF2400 exhibit exceptional large values for the mean hole volume and the width of the hole volume distribution, which may be attributed to the special structure of the AF copolymers discussed already above and in ref 27. The different conformations of the main chain and different distortion of the flat shape of the ring[61] and the bulky nature of the exocyclic $-CF_3$ groups are likely to bring a highly amorphous nature to this copolymer and to cause large nonthermal density fluctuations which are detected by PALS as a wide distribution of local free volumes. The occurrence of exceptional large holes in the glassy phase of AF 2400, compared with AF1600 (65 mol % dioxole with average sequence length of <2), might be attributed to the large fraction and the increased length (in average 6.7) of dioxole sequences in this material which contains 87 mol % of the dioxole.

The hole volume at T_g follows approximately a linear function of T_g, $\langle v_h(T_g)\rangle = \langle v_{hg}\rangle$ (Å^3) $= -450(\pm100) + 2.11\ (\pm0.3)T_g$ (K). The same is valid for $\sigma_h(T_g) = \sigma_{hg}$ where we found σ_{hg} (Å^3) $= -386(\pm90) + 1.46(\pm0.2)T_g$ (K). The extrapolated $\langle v_{hg}\rangle$

Table 3. Results from the Analysis of the PALS Experiments[a]

quantity	unc	PFE	CYTOP	AF1600	AF2400
T_g (K)	±5	265	377	438	∼505
$\langle v_{hg}\rangle$ (Å^3)	±3	163	248	470	665
σ_{hg} (Å^3)	±4	42	92	250	390
α_{hg} (10^{-3} K^{-1})	±0.2	2.18	1.87	0.37	0.16
α_{hr} (10^{-3} K^{-1})	±0.5	17.8	7.97	6.58	∼2.5
$dV/d\langle v_h\rangle$ (10^{21} g^{-1})		0.169 ± 0.003	0.194 ± 0.008	0.192 ± 0.006	0.33 ± 0.04
V_{occ}(PALS) (cm^3/g)		0.4389 ± 0.001	0.458 ± 0.003	0.482 ± 0.004	(0.3876 ± 0.03)
$dV_f/d\langle v_h\rangle$ (10^{21} g^{-1})		0.146 ± 0.003	0.206 ± 0.005	0.198 ± 0.005	0.312 ± 0.03
V_{f0} (cm^3/g)		0.0086 ± 0.0001	0.011 ± 0.002	0.030 ± 0.003	(−0.03 ± 0.03)
N_h' (10^{21} g^{-1})	±0.02	0.20 ± 0.01[b]	0.225 ± 0.005[b]	0.255 ± 0.01[c]	0.27 ± 0.01,[c] (0.24)[c,d]
N_h (nm^{-3})	±0.04	0.42[b]	0.46[b]	0.45[c]	0.44,[c] (0.42)[c,d]

[a] Shown are the mean, $\langle v_{hg}\rangle$, and the mean dispersion, σ_{hg}, of the hole volume distribution $g_n(v_h)$ at T_g(PALS), the coefficients of thermal expansion of the hole volume $\alpha_{hi} = (1/\langle v_{hg}\rangle)d\langle v_h(T)\rangle/dT$, where $i = g$ denotes the glass (at $T \rightarrow T_g$, $T < T_g$) and $i = r$ the rubber (at $T \rightarrow T_g$, $T > T_g$), the slopes $dV/d\langle v_h\rangle$, $dV_f/d\langle v_h\rangle$, and intersections with the y-axis V_{occ}((PALS) (cm^3/g) and V_{f0} (cm^3/g) of the V vs $\langle v_h\rangle$ (Figure 11) and V_f vs $\langle v_h\rangle$ (Figure 12) plots, the mean specific hole density estimated from Figure 13, and the mean volume related hole density, $N_h = N_h'/V$. [b] At 296 K. [c] At T_g. [d] Calculated from the corrected V_f.

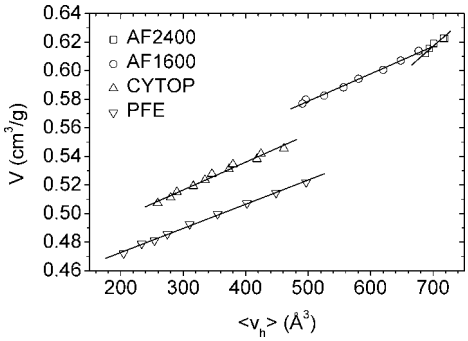

Figure 11. Specific total volume $V(T)$ from the temperature range above T_g plotted vs the mean hole volume $\langle v_h(T)\rangle$ for various fluoropolymers. The lines are linear fits to the data.

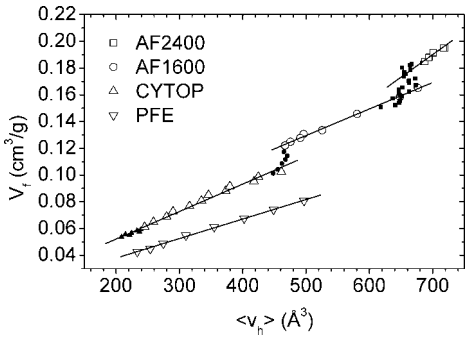

Figure 12. Specific hole free volume $V_f(T) = h(T)V(T)$ calculated from the S−S eos plotted vs the mean hole volume $\langle v_h(T)\rangle$ from PALS for various fluoropolymers. The empty symbols show the data from above T_g and the filled symbols from below. The lines are linear fits to the data from above T_g.

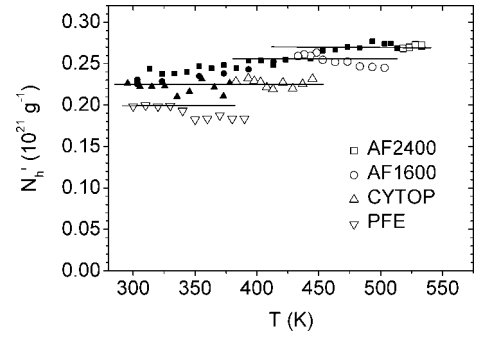

Figure 13. Calculation of the hole density from the relation $N_h'(T) = V_f(T)/\langle v_h(T)\rangle$ where $V_f(T) = h(T)V(T)$ comes from the S−S eos and $\langle v_h(T)\rangle$ from PALS. The filled and open symbols show values calculated for the glassy and rubbery states, respectively. The lines are a guide for the eyes.

starts at ∼215 K and σ_{hg} slightly higher, ∼270 K. Both dependences are distinctly steeper than observed for conventional polymers. For these polymers, which contain together with carbon and hydrogen only oxygen, nitrogen, or chlorine, we have analyzed $\langle v_{hg}\rangle$ (Å^3) = 17(±15) + 0.22(±0.05)T_g (K) or, more roughly, $\langle v_{hg}\rangle$ (Å^3) ≈ 0.27 T_g (K),[48] in agreement with previous estimations.[32] The corresponding relation for σ_{hg} is σ_{hg} (Å^3) = −15(±15) + 0.16(±0.05)T_g (K) or σ_{hg} (Å^3) ≈ 0.12 T_g (K). Thus, the increase of $\langle v_{hg}\rangle$ and σ_{hg} with T_g for our polymers is by 1 order of magnitude larger than for conventional polymers. We remark that the fluoroelastomer VDF/HFP22 (not shown, see ref 36) behaves like the conventional polymers and that PFE has an only slightly larger value than this group of polymers. Obviously, the particular behavior of CYTOP and the AF polymers is not mainly related to the occurrence of fluorine atoms but to heterocyclic units containing fluorine which form strong barriers against rotation around the chain axis.[61] Or, in other words, the decrease in $\langle v_{hg}\rangle$ and σ_{hg} (and in the hole fraction h) when going from AF2400 via AF1600 to CYTOP can be explained by the increasing fraction of flexible $-C_2F_4-$ groups (from 0.13 to 0.35 and 0.5 mole fractions) and a corresponding reduction of barriers of rotation making the formation of more densely packed chain structure in the copolymers easier. In case of both AFs the reduction in the bulky exocyclic CF_3 content plays a further role.

We remark here also that AF copolymers exhibit extraordinary broad lifetime distributions with ratios $\sigma_{hg}/\langle v_{hg}\rangle$ of 0.53 and 0.59, while CYTOP and PFE show ratios of 0.27 and 0.26. These larger values occur also in the glass at room temperature, in agreement with molecular modeling of the free volume structure by Hofmann et al.[13] for both AFs. These simulations show a wide distributions of holes assumed to be probed by *o*-Ps with large hole volumes and fractions in contrast to conventional glassy polymers. These results indicate the importance of nonthermal density fluctuations (concentration and conformational fluctuations) in AF materials. The volume parameters for both polymer groups correlate with the results of permeability studies.[13] Certain differences in the shape of the distributions derived from experiment and simulation were already discussed in the first part of our work.[27]

The coefficients of thermal expansion of the hole volume, α_h, shown in Table 3, are approximately 1 order of magnitude larger than the corresponding parameters of the total volume. While the thermal expansivities, $e_h = d\langle v_h\rangle/dT$, for our fluoropolymers are very comparable, the α_h values decrease distinctly when going from PFE to AF2400. This behavior is due to the large increase of the hole volume at T_g, $\langle v_{hg}\rangle$. A comparison of Figures 6 and 9 shows that the mean hole volume

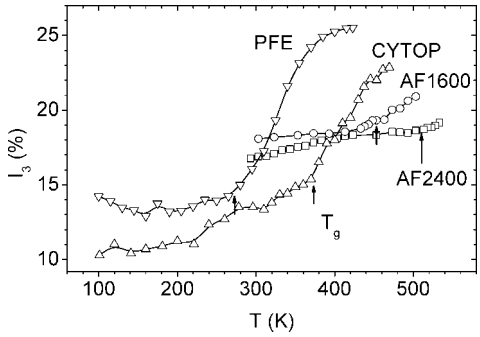

Figure 14. Relative intensity of the *o*-Ps lifetime component, I_3, as a function of the temperature T for various fluoropolymers.[27,36,38]

$\langle v_h(T)\rangle$ from PALS behaves in a parallel manner to the hole fraction $h(T)$ derived from PVT experiments. In case of AF2400 the behavior of $\langle v_h(T)\rangle$ seems to correspond to the corrected h values rather than to those derived directly from the S−S eos.

For an estimation of the hole density we made plots of total volume V vs $\langle v_h\rangle$ (Figure 11) for the data from above T_g and compare them with free volume, $V_f = hV$ vs $\langle v_h\rangle$, plots (Figure 12). One observes that the slopes in both plots, $dV/d\langle v_h\rangle$ and $dV_f/d\langle v_h\rangle$, agree sufficiently (Table 3). The plots $V_f = hV$ vs $\langle v_h\rangle$ go through zero, $\langle v_h\rangle = 0$, in most cases at positive free volumes, $V_{f0} > 0$. In these cases the fitted occupied volume, V_{occ}, is larger than V_{occ} from the S−S eos (Table 2). The data suggest $V_{occ}(\text{PALS}) = V_{occ}(\text{S−S eos}) + V_{f0}$. The slopes for AF2400 are distinctly larger than for the other fluoropolymers which we attribute largely to the inaccuracy of $\langle v_h\rangle$ owing to the small fitted temperature range which extends not much beyond T_g. Here the fits deliver $V_{f0} < 0$ and $V_{occ}(\text{PALS}) < V_{occ}(\text{S−S eos})$.

Notably is the deviation of the data from the glassy state from those of the rubbery in the plot of V_f vs $\langle v_h\rangle$ for both AFs. It comes from the fact that in the glass the hole volume $\langle v_h\rangle$ from PALS expands less than the specific hole free volume V_f from the S−S eos. This behavior is not observed for CYTOP and all other polymers we have studied in the past.

When linear plots of $V_f = hV$ vs $\langle v_h\rangle$ do not go through zero, i.e. $V_{f0} \neq 0$, the slope $dV_f/d\langle v_h\rangle$ does not agree with the hole density N_h'. This may indicate that some of our assumptions and ideas seem not to correspond to the reality. There are several reasons which can cause such a behavior: (i) *o*-Ps detects not the same volume as calculated from the S−S eos, (ii) the hole volume does not expand in three dimensions,[38,39] (iii) the weighting of the hole sizes distribution discussed previously is wrongly assumed or may change with temperature or size of holes, respectively, (iv) the hole density is not constant, and perhaps further reasons. The more or less agreement of the slopes $dV/d\langle v_h\rangle$ and $dV_f/d\langle v_h\rangle$, although $V_{f0} \neq 0$ (Table 3), might be considered as indication that item i does not describe the real reason for the unexpected behavior. The effect of the other items are difficult to distinguish.

A varying hole density may be easily handled by calculating N_h' for each couple (T, P) from

$$N_h'(T,P) = V_f(T,P)/\langle v_h(T,P)\rangle \quad (6)$$

In order to test these dependencies we have plotted in Figure 13 the hole density calculated from eq 6. When we tentatively assume for our discussion that N_h' should behave constant, then the apparent decrease of N_h' for PFE is an artifact, which may come from a weighting of hole sizes by the *o*-Ps probe larger than the assumed $v_h \sim r_h^3$, as it has been concluded in a previous work.[36] The apparent increase of N_h' for both AFs may be then the effect of a weighting factor of less than r_h^3. The behavior of the *o*-Ps intensity I_3, shown in Figure 14, may suggest such a behavior.

Some of us found in the past that above T_g frequently a certain temperature (and pressure) range appears in which I_3 varies parallel to τ_3. From this it was concluded that larger holes promote Ps formation.[37] The flattening of the increase of I_3 with increasing temperature and mean hole size $\langle v_h\rangle$, when going from PFE, via CYTOP, and AF1600 to AF2400 may indicate that the weighting decreases with increasing hole size from $\sim r_h^3$ (or even steeper) to a flatter dependence and may finally level off (compare Figures 14 and 9). Possible reasons for such a behavior were discussed in detail in ref 37.

From the plots in Figure 13 we have finally estimated the hole densities at T_g (or at 300 K). Table 3 shows the results. N_h' varies between 0.20 and 0.27 in units of 10^{21} g^{-1}, while the volume related hole density, $N_h = N_h'/V = h/\langle v_h\rangle$, lies between 0.42 and 0.46 nm^{-3}. When using the corrected specific free volume for the calculation of the hole density of AF2400, its value lowers slightly. These values for N_h' and N_h are smaller than those for conventional polymers. For these materials the hole density at T_g, N_{hg}, follows the relation N_{hg} (nm^{-3}) = $2.0(\pm 0.1) \times 10^{-3} T_g$ (K) (see also ref 32). That means N_h increases from 0.4 to 1 nm^{-3} when T_g varies from 200 to 500 K. Thus, the *o*-Ps probe detects in fluoropolymers containing heterocyclic rings a smaller number but of distinctly larger local free volumes than in conventional polymers.

Conclusions

The PVT data of amorphous Teflon AF1600 and AF2400 can be well fitted by the empirical Tait equation in the whole range of temperatures and pressures when the parameter C is allowed to be a fit parameter. The fits deliver two sets of, each of six, parameters for the temperature ranges below and above T_g. The fits of the S−S eos, which contains only three (scaling) parameters to the experimental volumes at ambient pressure (above T_g), are good; however, larger deviations are observed for medium pressures and higher temperatures.

The hole free volume fraction h derived from the S−S eos shows exceptional large values for both AF polymers: at room temperature the hole fraction amounts to $h = 0.186$ (AF1600) and 0.272 (AF2400) compared with 0.11 for the CYTOP and the fluoroelastomer PFE. The total (van der Waals) free volume fraction, $f_{total} = 1 - V_w/V$, of the AFs amounts to 0.438 and 0.460, respectively. The hole fraction h increases with temperature, for AF2400 to $h = 0.37$ at 600 K.

The mean and width of the hole volume distribution derived from the PALS data, $\langle v_h\rangle$ and σ_h, show—in good correlation with the h parameter—exceptional large values: at room temperature $\langle v_h\rangle$ amounts to 450 and 640 Å^3, σ_h amounts to 180 and 360 Å^3 for AF1600 and AF2400, respectively. For CYTOP and PFE the corresponding values are ∼220 and ∼80 Å^3. All of the parameters, V, h, $\langle v_h\rangle$, and σ_h, show a distinct increase in its gradient at the glass transition. The volume parameters at T_g, $\langle v_{hg}\rangle$, σ_{hg}, and h_g show certain (approximately linear or quadratic) variations with the value of T_g or the mass of the S−S mer, M_0. These dependencies exhibit for both AF polymers a distinctly larger gradient than found for all other polymers. This particularity of the AFs may be caused by their large fractions of the heterocyclic dioxole structure, each containing two bulky, exocyclic, CF_3 substituents.

From a comparison of PALS and PVT data the hole density was estimated to be almost constant at $N_h = h/\langle v_h\rangle = 0.42-0.46$ nm^{-3} for all of the fluoropolymers under discussion. This is smaller than for conventional polymers where N_h increases from 0.3 to 1.0 nm^{-3} when T_g varies from 200 to 500 K. Thus, the *o*-Ps probe detects in fluoropolymers containing heterocyclic

rings a smaller number but of distinctly larger local free volumes than in conventional polymers. This is particularly true for the Teflon AFs.

Acknowledgment. The authors acknowledge Yu. P. Yampolskii (Moscow) for stimulating discussions and helpful comments. We thank L. Häussler for the DSC analysis and H. Kunath (both Dresden) for the technical assistance in PVT experiments.

References and Notes

(1) Resnick, P. R.; Buck, W. H. In *Modern Fluoropolymers: High Performance Polymers for Diverse Applications*; Scheirs, J., Ed.; Wiley: Chichester, 1997; p 397.
(2) Nemser, S. M.; Roman, I. A. US Patent 5,051,114, 1991.
(3) Pinnau, I.; Toy, L. G. *J. Membr. Sci.* **1996**, *109*, 125.
(4) Alentiev, A. Yu.; Yampolskii, Yu. P.; Shantarovich, V. P.; Nemser, S. M.; Plate, N. A. *J. Membr. Sci.* **1997**, *126*, 123.
(5) Navarrin, W.; Tortelli, V.; Zedda, A. U.S. Patent 5,710,345, **1998**.
(6) Tanio, N.; Koike, Y. *Polym. J.* **2000**, *32*, 43.
(7) Ronova, I. A.; Rozhkov, E. M.; Alentiev, A. Yu.; Yampolskii, Yu. P. *Macromol. Theory Simul.* **2003**, *12*, 425.
(8) Nagel, C.; Günter-Schade, K; Fritsch, D.; Strunsky, T.; Faupel, F. *Macromolecules* **2002**, *35*, 2071.
(9) Dlubek, G.; Kilburn, D.; Alam, M. A. *Electrochim. Acta* **2004**, *49*, 5241.
(10) Bamford, D.; Reiche, A.; Dlubek, G.; Alloin, F.; Sanchez, J.-Y.; Alam, M. A. *J. Chem. Phys.* **2003**, *118*, 9420.
(11) Schmitz, H.; Müller-Plathe, F. *J. Chem. Phys.* **2000**, *112*, 1040.
(12) Nagel, C.; Schmidtke, E.; Günther-Schade, K.; Hofmann, D.; Fritsch, D.; Strunsky, T.; Faupel, F. *Macromolecules* **2000**, *33*, 2242.
(13) Hofmann, D.; Entrialgo-Castano, M.; Lebret, A.; Heuchel; Yampolskii, M. Y. *Macromolecules* **2003**, *36*, 8528.
(14) Cohen, M. H.; Turnbull, D. *J. Chem. Phys.* **1959**, *31*, 1164.
(15) Turnbull, D.; Cohen, M. H. *J. Chem. Phys.* **1970**, *52*, 3038.
(16) Jean, Y. C. In Positron Annihilation, Proc. of the 10th International Conference; He, Y.-J., Cao, B.-S., Jean, Y. C., Eds.; *Mater. Sci. Forum* **1995**, *175*, 59.
(17) Mogensen, O. E. *Positron Annihilation in Chemistry*; Springer-Verlag: Berlin, 1995.
(18) Pethrik, R. A. *Prog. Polym. Sci.* **1997**, *22*, 1.
(19) Bartoš, J. *Encyclopedia of Analytical Chemistry*; Meyers, R. A., Ed.; John Wiley & Sons Ltd.: Chichester, 2000; p 7968.
(20) Jean, Y. C., Mallon, P. E., Schrader, D. M., Eds.; *Principles and Application of Positron and Positronium Chemistry*; World Scientific: Singapore, 2003.
(21) Dlubek, G.; Kilburn, D.; Bondarenko, V.; Pionteck, J.; Krause-Rehberg, R.; Alam, M. A. *Macromol. Symposia, 210, Reactive Polymers 2003*; Adler, A.-J., Ed.; Wiley-VCH: Weinheim, 2004; p 11.
(22) Faupel, F.; Kanzow, J.; Günther-Schade, K.; Nagel, C.; Sperr, P.; Kögel, G. In Positron Annihilation, Proc. of the 13th International Conference (ICPA-13); Hyodo, T., Kobayashi, Y., Nagashima, Y., Saito, H., Eds.; *Mater. Sci. Forum* **2004**, *445*, 219.
(23) Zoller, P.; Walsh, C. J. *Standard Pressure-Volume-Temperature Data for Polymers*; Technomic Publ. Co.: Lancaster, Basel, 1995.
(24) Davies, W. D.; Pethrick, R. A. *Eur. Polym. J.* **1994**, *30*, 1289.
(25) Shantarovich, V. P.; Kevdina, I. B.; Yampolskii, Yu. P.; Alentiev, A. Yu. *Macromolecules* **2000**, *33*, 7453.
(26) Alentiev, A. Yu.; Shantarovich, V. P.; Merkel, T. C.; Bondar, V. I.; Freeman, B. D.; Yampolskii, Yu. P. *Macromolecules* **2002**, *35*, 9513.
(27) Rudel, M.; Kruse, J.; Rätzke, K.; Faupel, F.; Yampolskii; Yu., P.; Shantarovich, V. P.; Dlubek, G. *Macromolecules* **2008**, *41*, 788.
(28) Kansy, J. *Nucl. Instrum.Methods Phys. Res. A* **1996**, *374*, 235.
(29) Kansy, J. LT for Windows, Version 9.0, Inst. of Phys. Chem. of Metals, Silesian University, Bankowa 12, PL-40-007 Katowice, Poland, private communication, March **2002**.
(30) Dlubek, G.; Stejny, J.; Alam, M. A. *Macromolecules* **1998**, *31*, 4574.
(31) Bohlen, J.; Kirchheim, R. *Macromolecules* **2001**, *34*, 4210.
(32) Srithawatpong, R.; Peng, Z. L.; Olson, B. G.; Jamieson, A. M.; Simha, R.; McGervey, J. D.; Maier, T. R.; Halasa, A. F.; Ishida, H. *J. Polym. Sci., Part B: Polym. Phys.* **1999**, *37*, 2754.
(33) Schmidt, M.; Maurer, F. H. J. *Macromolecules* **2000**, *33*, 3879.
(34) Dlubek, G.; Bondarenko, V.; Al-Qaradawi, I. Y.; Kilburn, D.; Krause-Rehberg, R. *Macromol. Chem. Phys.* **2004**, *205*, 512.
(35) Kilburn, D.; Dlubek, G.; Pionteck, J.; Bamford, D.; Alam, M. A. *Polymer* **2005**, *46*, 869.
(36) Dlubek, G.; Sen Gupta, A.; Pionteck, J.; Krause-Rehberg, R.; Kaspar, H.; Lochhaas, K. H. *Macromolecules* **2004**, *37*, 6606.
(37) Dlubek, G.; Wawryszczuk, J.; Pionteck, J.; Goworek, T.; Kaspar, H.; Lochhaas, K. H. *Macromolecules* **2005**, *38*, 429.
(38) Dlubek, G.; Pionteck, J.; Sniegocka, M.; Hassan, E. M.; Krause-Rehberg, R. *J. Polym. Sci., Part B: Polym. Phys.* **2007**, *45*, 2519.
(39) Consolati, G.; Quasso, F.; Simha, R.; Olson, G. B. *J. Polym. Sci., Part B: Polym. Phys.* **2005**, *43*, 2225.
(40) Nanda, V. S.; Simha, R. *J. Chem. Phys.* **1964**, *21*, 1884.
(41) Simha, R.; Somcynsky, T. *Macromolecules* **1969**, *2*, 342.
(42) Robertson, R. E. In *Computational Modeling of Polymers*; Bicerano, J., Ed.; Marcel Dekker: Midland, MI, 1992; p 297.
(43) Utracki, L. A.; Simha, R. *Macromol. Theory Simul.* **2001**, *10*, 17.
(44) Zoller, P. In *Polymer Handbook*, 3rd ed.; Brandrup, J., Immergut, E. H., Eds.; J. Wiley & Sons: New York, 1989.
(45) Rogers, P. A. *J. Appl. Polym. Sci.* **1993**, *48*, 1061 and 2075.
(46) De Angelis, M. G.; Merkel, T. C.; Bondar, V. I.; Freeman, B. D.; Doghieri, F.; Sarli, G. C. *Macromolecules* **2002**, *25*, 1276.
(47) Van Krevelen, D. W. *Properties of Polymers*; Elsevier Sci. Publ. Co.: Amsterdam, 1993.
(48) Dlubek, G. Local free volume distribution from PALS and dynamics of polymers, to be published.
(49) Zoller, P.; Jain, R. K.; Simha, R. *J. Polym. Sci., Part B: Polym. Phys.* **1986**, *24*, 687.
(50) Jain, R. K.; Simha, R. *J. Polym. Sci., Polym. Phys. Ed.* **1982**, *20*, 1399.
(51) Simha, R.; Carri, G. *J. Polym. Sci., Part B: Polym. Phys.* **1994**, *32*, 2645.
(52) Dlubek, G.; Pionteck, J. Proceedings of the 38th Polish Seminar on Positron Annihilation. *Acta Phys. Pol.* **2008**, *113*, 1331.
(53) Simha, R.; Wilson, P. S. *Macromolecules* **1989**, *6*, 908.
(54) Schrader, D. M.; Usmar S. G. In *Positron Annihilation in Fluids*; Sharma, S. C., Ed.; World Scientific: Singapore, 1988; p 215.
(55) Gregory, R. B. *J. Appl. Phys.* **1991**, *70*, 4665.
(56) Tao, S. J. *J. Chem. Phys.* **1972**, *56*, 5499.
(57) Eldrup, M.; Lightbody, D.; Sherwood, J. N. *Chem. Phys.* **1981**, *63*, 51.
(58) Nakanishi, H.; Wang, S. J.; Jean, Y. C. In *Positron Annihilation Studies of Fluids*; Sharma, S. C., Ed.; World Scientific: Singapore, 1988; p 292.
(59) Liu, J.; Deng, Q.; Jean, Y. C. *Macromolecules* **1993**, *26*, 7149.
(60) Dlubek, G. *J. Non-Cryst. Solids* **2006**, *352*, 2869.
(61) Tokarev, A. V.; Bondarenko, G. N.; Yampolskii, Yu. P. *Polym. Sci., Ser. A* **2007**, *49*, 909.

MA800748A